J11.4

GROUND BASED APPROACH TO DIRECT EVALUATION OF AEROSOL-CLOUD INTERACTION

Yuzhe He, Bomidi Madhavan, Lina Cordero, Yonghua Wu, Barry Gross*, Fred Moshary, Sam Ahmed
The City College of the City University of New York

Abstract. The quantification of the first direct aerosol cloud interaction mechanism requires simultaneous observations of cloud water drop properties as well as aerosol properties below the cloud. The simultaneous measurement of both these properties is very difficult from space borne systems and efforts to develop ground remote sensing measurements are critical. To measure the cloud properties, we make use of an approach which combines a Microwave radiometer and a MFRSR radiometer for simultaneous Cloud Optical Depth (COD) and Liquid Water Path (LWP). From these measurements, effective droplet diameter can be estimated assuming the homogeneity of the cloud. Unfortunately, for thin clouds, COD measurements from the MFRSR are often underestimated due to strong forward scattering of radiation in the solar aureole region which is blocked and therefore not contained within the MFRSR diffuse measurements. However, by suitable calculation, we can estimate the fractional radiation within the shadow region as a function of cloud properties directly and find that for COD > 2 and solar zenith angles < 60, the standard MFRSR correction can be applied with errors < 1%. Also, we discuss the uncertainty in the inferred COD due to various input parameters in the formation of Look-Up-Tables and future insight in overcoming these uncertainty issues is presented.

1. INTRODUCTION

Aerosols have important impact on cloud formation by acting as the cloud condensation nuclei (CCN) in the atmosphere. The aerosol indirect effect [Twomey et al., 1984] indicates that increasing aerosol particle number concentration correlates to decreasing droplet size and increasing cloud reflectance. Satellite measurements have shown that urban pollution causes a shift to smaller droplet sizes and more cloud droplets [Twohy et al., 1995; Kaufman and Fraser, 1997; Wetzel and Stowe, 1999; Kaufman et al., 2005]. However, the relationship between aerosols and clouds in the urban region is not as significant as over ocean [Jin and Shepherd, 2008].

Current understanding of aerosol effects on clouds is far from complete. In addition to aerosol temporal and spatial variation, the complexity of aerosol-cloud interaction in urban region is due to the local dynamics and thermodynamics. One of the biggest challenges in assessing the aerosol effects on clouds is obtaining the temporal and spatial observation for aerosol and clouds simultaneously. In general, remote sensing techniques cannot measure aerosols when clouds are present. To overcome this problem, the statistical analysis method is used.

Corresponding author address: Barry Gross, EE Dept., The City College of New York, CUNY, New York, NY 10031; e-mail: gross@ccny.cuny.edu

Any approach requires aerosol measurements near the cloud base and direct measurement of cloud droplet effective radius in the cloud layer. Since the change of effective radius versus aerosol loading is obtained for a fixed liquid water path (LWP), measuring LWP will reduce the uncertainty in the inferred cloud optical properties. In this study, we briefly discuss the concerning aspects related to satellite based approach for cloud retrievals and the methodology for ground based retrieval. Also, the sensitivity of various parameters used for inferring COD are discussed and future direction to reduce the uncertainty aspects are indicated.

2. SATELLITE BASED APPROACH

2.1 *The Theoretical Basis*

The simple adiabatic model [Duynkerke et al., 1995; Pawlowska and Brenguier, 2000] for the liquid water content (LWC) can be expressed as:

$$w(h) = c_w h \tag{1}$$

where $w(h)$ is the cloud liquid water content in kg/m^3, c_w is the condensation rate in kg/m^4, and h is the height in meters above the cloud base. Since the condensation rate is subject to excess water vapor, it is primarily dependent on the temperature. Because marine boundary layer

clouds are shallow with little temperature variation, the condensation rate can be considered as constant. Therefore, the total liquid water path (LWP) can be represented simply as the integral of the liquid water content of the cloud:

$$W = \frac{1}{2} c_w H^2 \qquad (2)$$

where W is the liquid water path in kg/m^2 and H is the cloud geometrical thickness in meters.
In the adiabatic cloud model, the optical thickness of a cloud can be related to cloud droplet number concentration, N, and geometrical thickness, H as:

$$\tau = \frac{3}{5}\pi Q \left[\frac{3c_w}{4\pi\rho_L}\right]^{2/3} [kN]^{1/3} H^{5/3} \qquad (3)$$

where Q is the scattering efficiency (≈ 2) and $k = \left(r_v / r_{eff}\right)^3$ is the ratio between the volume mean radius and the effective radius, ρ_L, τ, r_{eff} are the density of liquid water, cloud optical thickness and cloud droplet effective radius, respectively. From equation (2) and (3) the cloud geometrical thickness and cloud droplet number concentration can be expressed as:

$$H = \left[2\frac{W}{c_w}\right]^{1/2} \qquad (4)$$

$$N = \frac{2^{-5/2}}{k}\tau^3 W^{-5/2}\left[\frac{3}{5}\pi Q\right]^{-3}\left[\frac{3}{4\pi\rho_L}\right]^{-2} c_w^{1/2} \qquad (5)$$

Equation (5) allows us to derive the cloud droplet number concentration from MODIS cloud product.

2.2 *The Date Sets*

Moderate Resolution Imaging Spectroradiometer (MODIS) is a multi-channel visible and infrared imaging radiometer deployed on board both Aqua and Terra satellites. MODIS has 36 bands ranging from 0.415um to 14.285um. The spatial resolutions are 250m for band 1 and 2, 500m for band 3 to 7, and 1000m for band 8 to 36. In this study, we used 2009 MODIS level 2 (collection 5) data derived from Terra. We obtained the aerosol optical depth (AOD) from MOD04_L2. The cloud droplet number concentration is calculated from MOD06_L2 by using equation (5). In this investigation, we focused on the 1 degree by 1 degree area centered at New York City.
In order to obtain the low-level warm clouds, several constraints were applied. The cloud pixel was selected with cloud type flag of water, a cloud probability greater than 50%, cloud top temperature greater than 273K, and cloud optical thickness greater than 3.

2.3 *The Results*

In figure 1, the cloud droplet number annual trend is plotted. We note similar seasonal cloud droplet number concentration variation in Northeastern U.S. in [Han et al., 1998; Rausch et al., 2010] where the highest value of the cloud droplet number concentration was found in winter and spring. However, the AOD has an opposite trend. Both MODIS AOD product and AERONET measurement suggest that the summer has highest total AOD shown in figure 2 thereby implying a somewhat inverse relationship between AOD and particle number which seems counterintuitive. However, when the AOD was separated into fine mode and coarse mode, we found that coarse mode AOD has higher values than fine mode AOD in spring and winter.

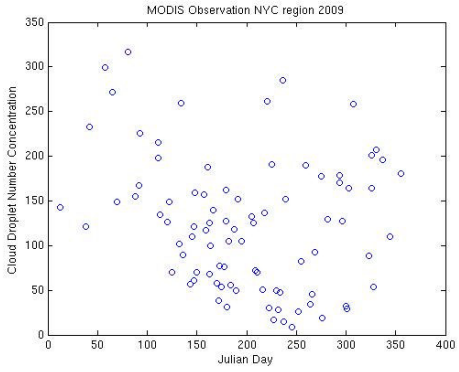

Figure 1: Daily cloud droplet number concentration of 2009 inferred from MOD06_L2.

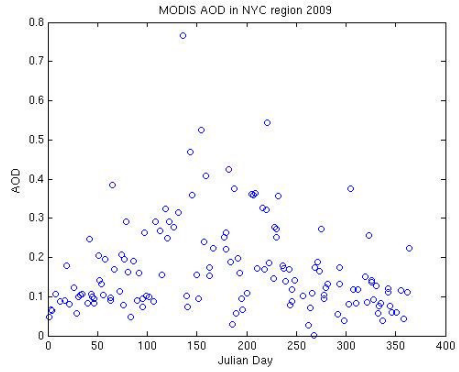

Figure 2: Daily AOD of 2009 from MOD04_L2.

Suggesting that the correlation between the aerosols and CCNs is stronger when considering the coarse mode. Figure 3 shows a seasonally binned regression of the aerosol optical thickness and cloud droplet number concentration for both fine and coarse mode. While the fine mode correlation clearly is not visible within our data, there is a weak correlation between coarse mode AOD and cloud droplet number.

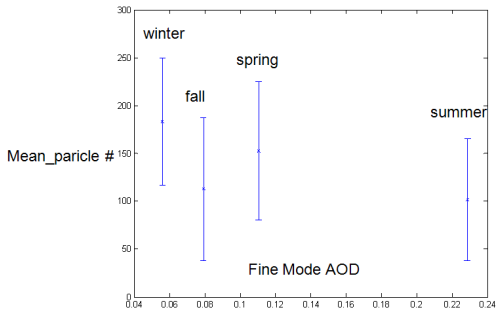

Figure 3(a): Fine mode AOD vs. mean particle numbers in four seasons of 2009.

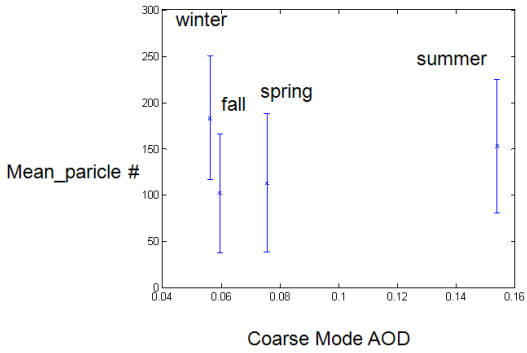

Figure 3(b): Coarse mode AOD vs. mean particle numbers in four seasons of 2009.

In making this conclusion, we ignored the winter results due both to the small data set obtained as well as modifications of the meteorological environment in winter due to the differences in the overall jet stream.

Clearly, such statistical measures are difficult to interpret so methods to extract aerosol-cloud properties on an individual cloud basis is needed and our efforts in this direction are described below.

3. GROUND BASED APPROACH

The Multi-Filter Rotating Shadowband Radiometer (MFRSR) is a ground based instrument which makes simultaneous measurements of solar irradiances at six passband wavelengths centered at 411.5, 496.7, 614.3, 670.6, 865.1 and 936.7 nm. It works on the principle of 'blocking mechanism' [Harrison et al., 1994] to obtain instantaneously direct-normal, total-horizontal and diffuse-horizontal irradiance components for almost every minute. The capability of MFRSR to observe solar irradiances even under overcast skies gives scope for inferring cloud optical depth (COD). MFRSR can calculate thick unbroken cloud optical properties using diffuse horizontal flux measurements. However, the approach requires estimates of effective droplet radius (~ 20% errors are possible without accurate effective droplet radius). Thus, the need for simultaneous measurements of LWP from Microwave Radiometer (MWR) along with inferred COD from MFRSR irradiance observations would give the effective droplet radii (R_{eff}) in the cloud layer. Though this is an iterative approach where initially R_{eff} has to be assumed for COD retrievals and finally iterations are performed for convergence.

3.1 *Forward Scattering Correction*:

The band measures three times during a measurement cycle. First, the shadow band blocks the Sun with and umbral angle ($\Delta\Phi_B$) of 3.27 and polar angles from 0 to about 90 degrees. The remaining two off-center ($\pm$9 degree) measurements are taken to compensate for the excess sky that is blocked during the first measurement. Since the band at the position B_0 blocks some of the diffuse beam resulting in an underestimation of diffuse irradiance. In order to compensate this, a first order correction is implemented operationally where the band covers the sky $\pm$ 9 degrees away. The compensation assumes that part of the sky blocked at 9 degrees is equal to the diffuse irradiance observed at central blocking (B_0). Min et al. [2004] modified the DISORT radiative transfer code [Stamnes et al., 1988] by combining the δ-fit method with the Nakajima-Tanaka intensity correction procedure to accurately and rapidly compute radiances in both forward and backward directions.

Here we consider analytical expressions for total hemispheric diffuse flux ($I_{dif}^{\downarrow}$), diffuse flux in the blocked measurement (B_0) and average diffuse flux of two off-center ($\pm$ 9 degrees) measurements. $L_{\lambda}^{\downarrow}$ is the downwelling diffuse radiance as a function of cosine of view zenith angle μ and relative azimuth angle φ. Evaluating the integrals

defined below using the Gaussian Quadrature method, we have obtained

(a) Total hemispheric diffuse flux at the surface is given by

$$I_{dif}^{\downarrow} = \int_0^{2\pi} d\varphi \int_0^1 L_\lambda^{\downarrow}(\tau^*, -\mu, \varphi)\mu d\mu \qquad (6)$$

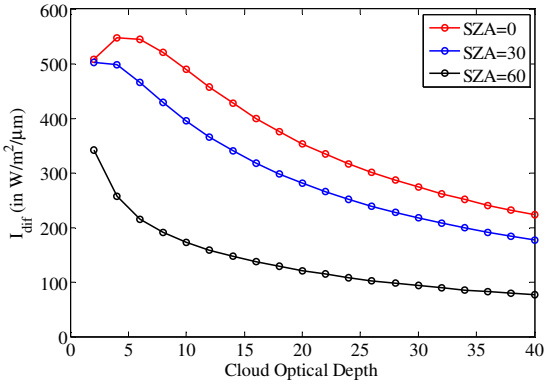

Figure 4(a): Total hemispheric diffuse irradiance as a function of COD for different SZA (0, 30 and 60 degrees)

(b) Blocked scattered radiation for middle measurement is given by

$$B_0 = \int_{\left(\frac{-\Delta\phi_B}{2}\right)}^{\left(\frac{+\Delta\phi_B}{2}\right)} d\varphi \int_0^1 L_\lambda^{\downarrow}(\tau^*, -\mu, \varphi)\mu d\mu \qquad (7)$$

(c) ± 9 degrees blocked scattered radiation on either side of the diffuser is given by

$$B_{se} = \int_{\left(\frac{-\Delta\phi_B}{2}\right)-9}^{\left(\frac{+\Delta\phi_B}{2}\right)-9} d\varphi \int_0^1 L_\lambda^{\downarrow}(\tau^*, -\mu, \varphi)\mu d\mu \qquad (8)$$

$$B_{sw} = \int_{\left(\frac{-\Delta\phi_B}{2}\right)+9}^{\left(\frac{+\Delta\phi_B}{2}\right)+9} d\varphi \int_0^1 L_\lambda^{\downarrow}(\tau^*, -\mu, \varphi)\mu d\mu \qquad (9)$$

(d) First order forward scattering correction is obtained by

$$\Delta I = B_0 - (B_{se} + B_{sw})/2 \qquad (10)$$

The figures 4(a) and 4(b) are the total hemispheric diffuse irradiance and first order forward scattering correction as a function of COD at SZA = 0, 30 and 60 respectively.

The figure 5 shows the fractional contribution of first order forward scattering correction in the total hemispheric diffuse irradiance as a function of cloud optical depths for SZA = 0, 30 and 60 degrees.

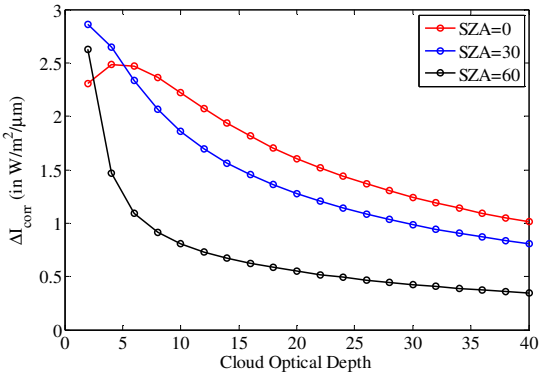

Figure 4(b): First order forward scattering correction in the diffuse irradiance as a function of COD for different SZA (0, 30 and 60 degrees)

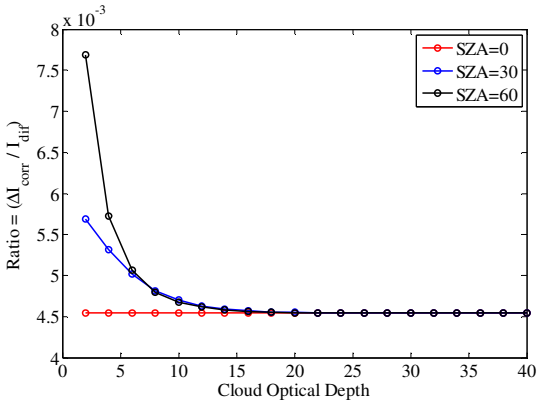

Figure 5: Fractional contribution of forward scattering correction in the diffuse irradiance at the surface as a function of COD for different SZA (0, 30 and 60 degrees)

It can be observed that the error in this assumption is significant for single scattering where the radiation is focused near the aureole but much less critical for high COD with massive multiple scattering correction factor.

3.2 *Method*

The Look-Up-Tables (LUTs) of downwelling diffuse irradiance using the SBDART plane parallel radiative transfer code as function of

cosine of SZA and CODs are generated for the chosen passband wavelength. The extraterrestrial solar irradiance on a horizontal plane parallel to the Earth's surface and perpendicular to the Sun rays is a function of cosine of SZA and the day of the year. Since there is negligible chance to infer extraterrestrial response from Langley regression on an overcast day, it is suggested for an interpolated value from those observed on clear days. Also, it is seen that the extraterrestrial response in the forenoon and afternoon varies on a clear day. Min and Harrison [1996] indicated that the uncertainty due extraterrestrial response introduced from Langley regression of MFRSR measurements at a difficult site is approx 5%.

So, here we confine our retrievals using diffuse horizontal irradiance observed at the surface instead of atmospheric transmittance. LUTs are generated by fixing the cloud layer at an altitude of 4-5 km with uniform cloud droplet radii (NRE = 20 micron), surface albedo (rg = 0.05), and column aerosol extinction (AOD = 0.5) for passband wavelength 411.5 nm. Since the surface albedo is less sensitive at lower wavelengths, we confine our retrievals to 411.5 nm passband.

Finally, calculate the instantaneous CODs from the MFRSR observed instantaneous diffuse irradiance as a function of cosine of SZA.

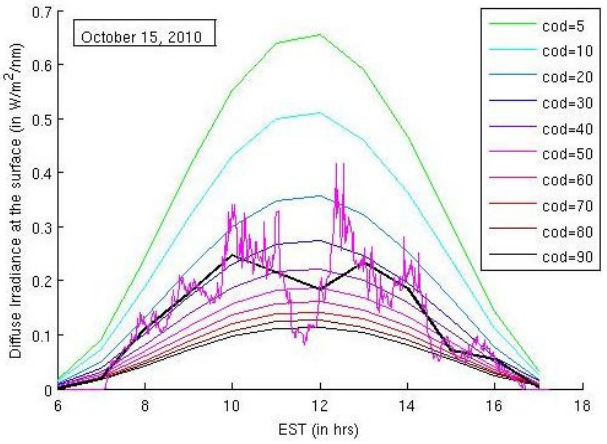

Figure 6: Look Up Table (LUT) of diffuse irradiance for different COD as a function of time in hours for October 15, 2010.

The calculation of CODs from observed diffuse irradiance using the LUT with as a function of time is shown in figure 6. Thick black line and magenta color lines are the 1-hour averaged and raw observed diffuse irradiance as a function of time respectively. It can be seen that the hourly averaged line reduces the noise in the raw data.

3.2 *Sensitivity Study*

The accuracy of inferred cloud optical properties is influenced by the following chosen parameters:

- Aerosol optical depth (AOD)
- Cloud drop effective radius (NRE)
- Surface albedo (rg)
- Aerosol humidification in the BLA model i.e., URBAN
- Altitude of cloud layer (ZCLOUD)

For quantitative assessment of errors due to input parameters, we choose the reference state of variable parameters namely, AOD = 0.5, NRE = 20 microns, COD = 20, rg = 0.05, SZA = 30 degrees, and RH = 80%. The sensitivity analysis is performed based on 10% perturbation of the parameters (i.e., using root mean square definition with equal errors on both sides) and the RMS errors for AOD, NRE, rg, RH are obtained as $\pm$ 5.26%, $\pm$ 0.65%, $\pm$ 0.41%, $\pm$ 14.41% respectively. The altitude of cloud layer irrespective of whether it is at 1-2 km or 4-5 km has negligible impact on the inferred CODs.

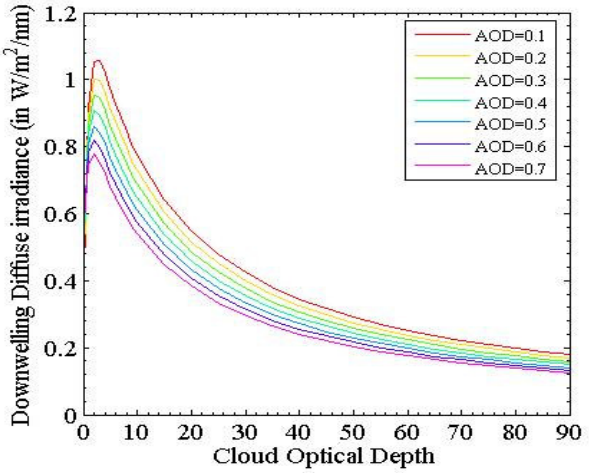

Figure 7(a): Downwelling diffuse irradiance as a function of COD for different aerosol loadings on an overcast day obtained from SBDART model

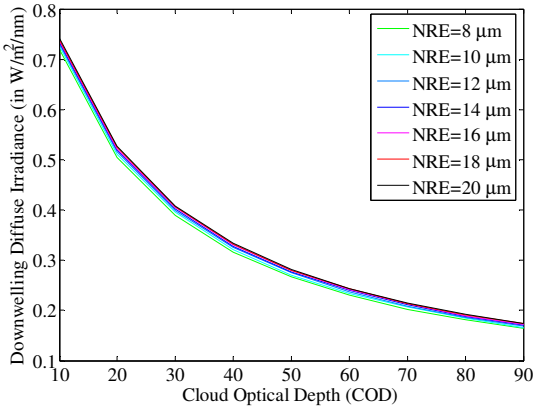

Figure 7(b): Downwelling diffuse irradiance as a function of COD for different cloud droplet effective radii (R_{eff} or NRE) obtained from SBDART model

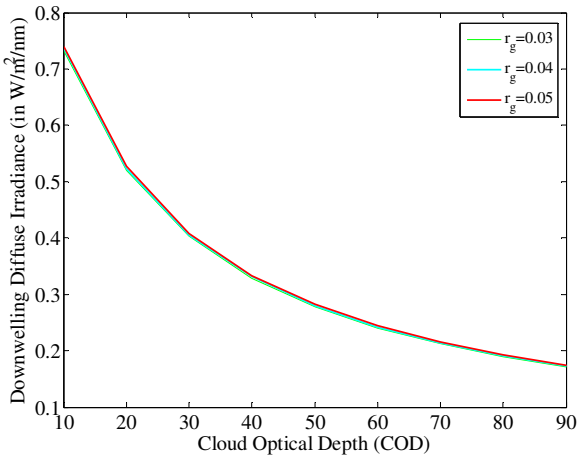

Figure 7(c): Downwelling diffuse irradiance as a function of COD for different surface albedos obtained using SBDART model

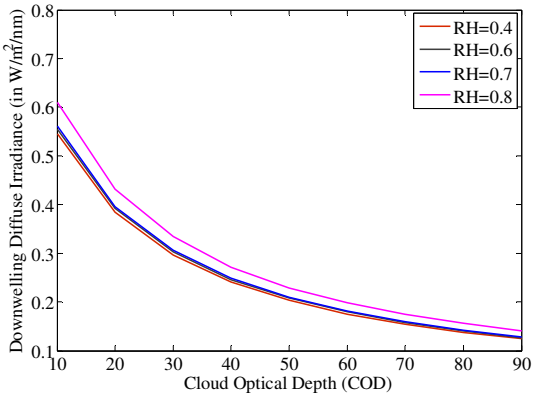

Figure 7(d): Downwelling diffuse irradiance as a function of COD for different surface RH in the Urban BLA model in the SBDART.

The figures 7(a) to 7(d) show the variation of downwelling diffuse irradiance as a function of CODs for varied AOD, NRE, rg and RH respectively.

In order to reduce the uncertainty induced by various parameters, we plan to use the RH observed by co-located Microwave Radiometer (MWR) in the BLA model. This would reduce the uncertainty due to absorption in the BLA model. Also, using the CODs from MFRSR and LWP (liquid water path) from MWR the cloud droplet effective radii (NRE) can be estimated. Surface albedo is less sensitive at lower wavelengths. So, using estimates of satellite surface albedo products like ASRVN will reduce the fractional uncertainty arising in the inferred CODs due to surface albedo.

4. FUTURE SCOPE

Microwave Radiometer (MWR) has undergone several preliminary tests including accurate path integrated total precipitable water against GPSMET and AERONET water vapor products. An example of such a comparison is seen in figure 8 where 1 hr binned averages between the MWR and AERONET column integrated water vapor are compared. We find that except for very low cases in winter, the results are unbiased with errors < 10%. A small positive bias is observed in winter but is probably due to calibration issues since the winter measurements were done over a longer period from the initial calibration.

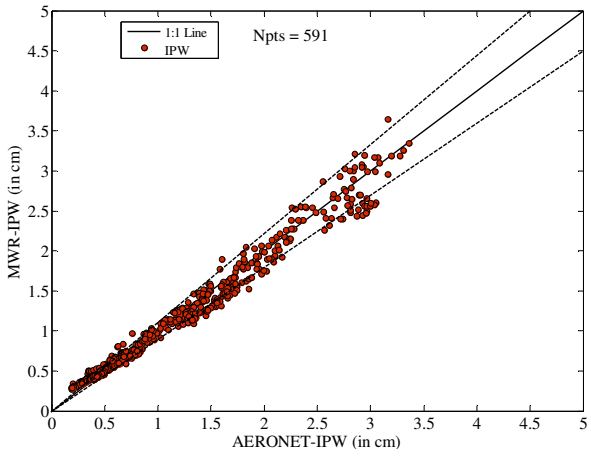

Figure 8 Hourly binned comparison of IPW between AERONET and MWR.

However, tests related to water vapor mixing ratio profiles (g/kg) using matchups from our Raman Lidar are still process. Also, we plan to implement direct flux algorithm of Min et al [2004] for low / broken cloud cases by choosing ratio of diffuse to direct flux as threshold. This case would enable us to better understand the aerosol-cloud effects for thin clouds.

Acknowledgement. This work is partially supported by the research projects of NOAA-CREST #NA17AE1625 and NOAA-ISET #NA06OAR4810187. The views, opinions and findings contained in this report are those of the author(s) and should not be construed as an official NOAA or U.S. Government position, policy, or decision.

REFERENCES:

Duynkerke, P., H. Zhang, and P. Jonker (1995), Microphysical and turbulent structure of nocturnal stratocumulus as observed during ASTEX, *J. Atmos. Sci., 52,* 2763-2777.

Han, Q., W. B. Rossow, J. Chou, R. M. Welch (1998), Global variation of column droplet concentration in low-level clouds, *Geophys. Res. Letters, Vol. 25, No. 9,* 1419-1422.

Harrison, L.C., J.J. Michalsky, and J. Berndt (1994), Automated multifilter rotation shadowband radiometer: An instrument for optical depth and radiation measurements, *Appl. Opt*., 33, 5188.

Jin, M., and J. M. Shepherd (2008), Aerosol relationship to warm season clouds and rainfall at monthly scales over east China: urban land versus ocean, *J. Geophys. Res., 113,* D24S90, doi: 10.1029/2008JD010276.

Kaufman, Y. J., and R. S. Fraser (1997), The effect of smoke particles on clouds and climate forcing, *Science, 277,* 1636-1639.

Min, Q., and Lee C. Harrison (1996), Cloud properties derived from surface MFRSR measurements and comparison with GOES results at the ARM SGP site, *Geophy. Res. Lett.,* 23, 13, 1641-1644.

Min, Q., E. Joseph, and M. Duan (2004), Retrieval of thin cloud optical depth from a multifilter rotating shadowband radiometer, *J. Geophys. Res.,* 109, D02201, doi: 10.1029/2003JD003964.

Pawlowska, H., and J. Brenguier (2000), Microphysical properties of stratocumulus clouds during ACE-2, *Tellus, Ser. B, 52,* 868-887

Rausch, J., A. Heidinger, R. Bennartz (2010), Regional assessment of marine boundary layer cloud microphysical properties using the PATMOS-x dataset, *J. Geophys. Res., 115,* D23212, doi:10.1029/2010JD014468.

Stamnes, K., S.-C. Tsay, W.J. Wiscombe, and K. Jayaweera (1988), Numerical stable algorithm for discrete-ordinate method radiative transfer in multiple scattering and emitting layered media, Applied Optics, 27, 2502-2509.

Twohy, C. H., P. A. Durkee, B. J. Huebert, and R. J. Charlson (1995), Effects of aerosol particles on the microphysics of coastal stratiform clouds, *J. Clim., 8,* 773-783.

Twomey, S. A., M. Piepgrass, and T. L. Wolfe (1984), An assessment of the impact of pollution on global cloud albedo, *Tellus, Ser. B,* 36, 356-366.

Wetzel, M. A., and L. L. Stowe (1999), Satellite-observed patterns in stratus microphysics, aerosol optical thickness and shortwave radiative forcing, *J. Geophys. Res., 104,* 31,287-31,299.